Electronic Supplementary Material (ESI) for Nanoscale.

Supporting Information

Voltage Driven Chemiresistor with Ultralow Power Consumption Based on Self-Heating Bridged WO_3 Nanowires

Tiantian Dai [a,b], , *Zanhong Deng* [b,d], *Meng Li* [b,d], *Shimao Wang* [b,d], *Mengxiao Chen* [a,c,*], *Gang Meng* [b,d,*]

[a] Research Center for Humanoid Sensing, Zhejiang Lab, Hangzhou 311100, China

[b] Anhui Provincial Key Laboratory of Photonic Devices and Materials, Anhui Institute of Optics and Fine Mechanics, and Key Lab of Photovoltaic and Energy Conservation Materials, Chinese Academy of Sciences, Hefei 230031, China

[c] College of Biomedical Engineering & Instrument Science, Zhejiang university, Hangzhou 311100, China.

[d] Advanced Laser Technology Laboratory of Anhui Province, Hefei 230037, China

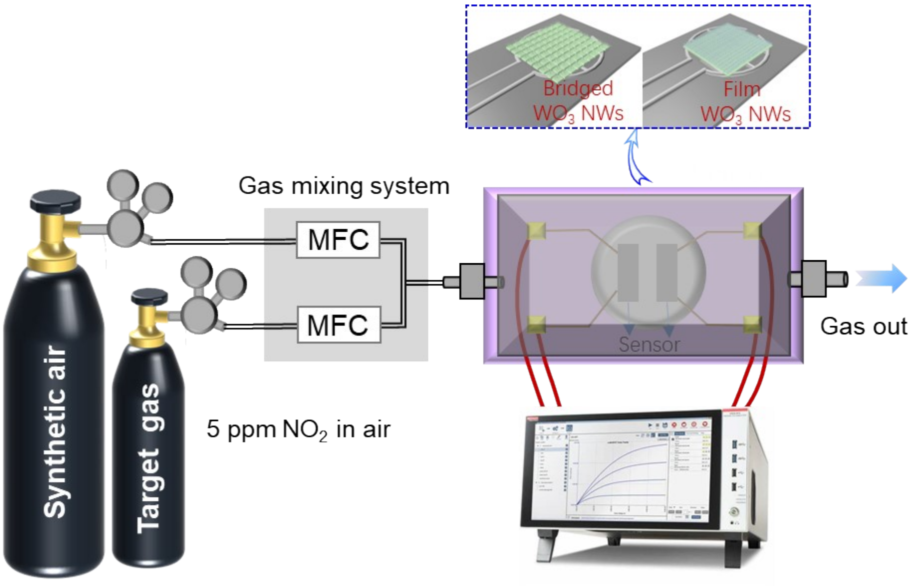

Figure S1. The schematic image of dynamic measurement system and the chemiresistor devices.

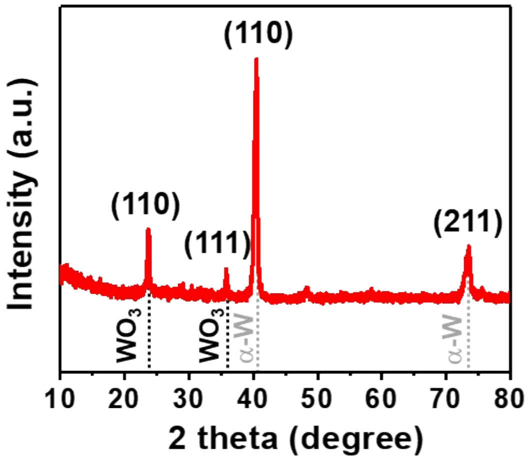

Figure S2. XRD of WO_3 nanowires prepared on quartz substrate.

The XRD of WO_3 nanowires after thermal oxidating $W_{18}O_{49}$ nanowires (prepared by thermal oxidating W film (~500 nm) in a oxygen-deficient atmosphere) in air at 500 ºC for 3 h is shown in Figure S2. The diffraction peak of W metal showed in XRD, revealed the incomplete oxidation of W film. The (110) at 23.68º and (111) peaks correspond to WO_3 nanowires. The (110) at 40.52º and (211) peaks correspond to W film. According to the Scherrer formula: $D = K\lambda / (\beta\cos\theta)$, in which K is constant, λ is wavelength of x-ray, β is the half height and width of diffraction peak, θ is diffraction angle, the grain size of WO_3 nanowires and W film are 15.5 nm and 16.9 nm, respectively.

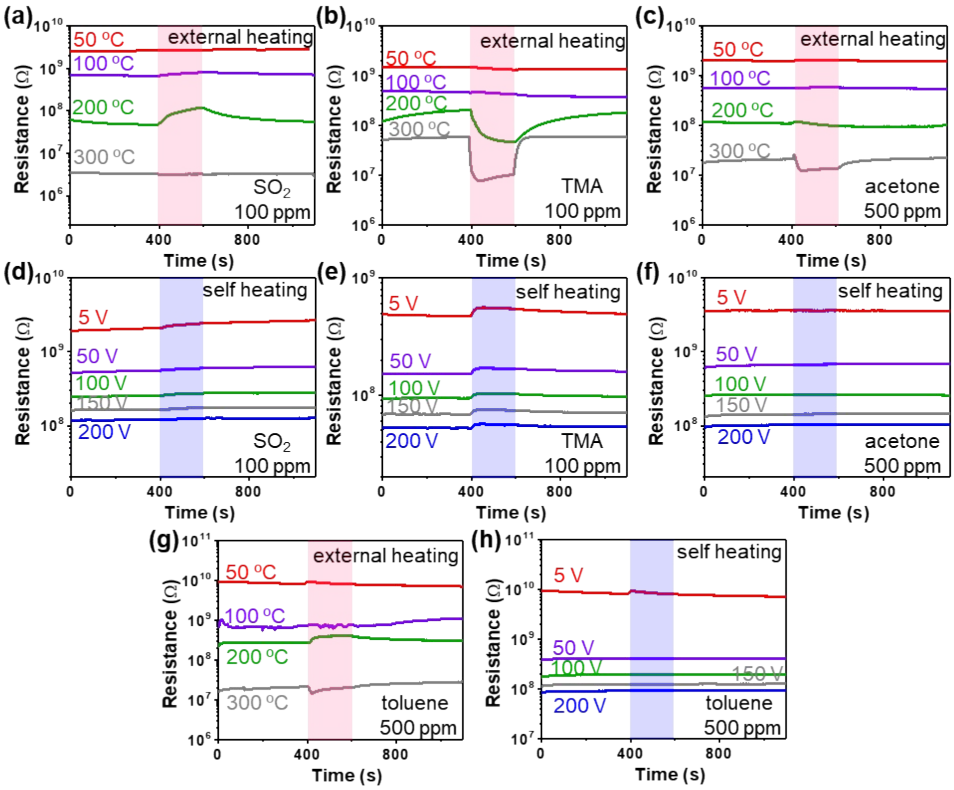

Figure S3. The responses of bridged WO_3 NWs to various gases under different heating modes. (a, d) SO_2, (b, e) TMA, (c, f) acetone, (g, h) toluene. The responses marked by pink rectangles and blue rectangles are operated on external heating mode and self-heating mode, respectively.

The bridged WO_3 NWs chemiresistor possesses a worse gas performance to aforementioned gases compared with NO_2.

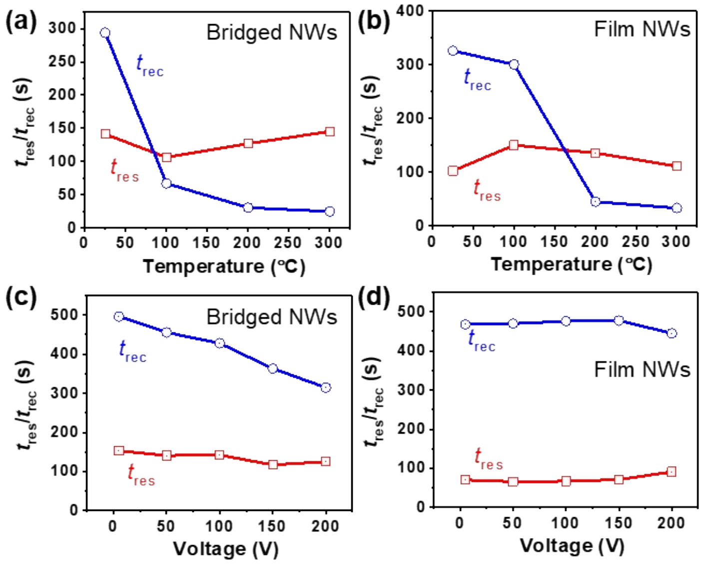

Figure S4. The response (t_{res}) and recovery time (t_{rec}) of bridged WO_3 NWs and WO_3 film NWs chemiresistors under different operation modes. (a, b) external heating mode, (c, d) self-heating mode.

Bridged NWs chemiresistor (Figure S3a) exhibits similar response kinetics with film NWs chemiresistor (Figure S3b) under external heating mode, inferring a slight variation of gas/ MOS-surface redox events between the bridegd structure and film structure. For self-heating mode, the bridged NWs chemiresistor possesses similar response kinetics with external mode and the t_{rec} decrease with the increase of applied voltage, implying the temperature of nanojunction of bridged NWs increase induced by joule heat with the increase of applied voltage. Inversely, there is no obvious change for t_{rec} and t_{rev} of film NWs chemiresistor with the increase of applied voltage, implied little joule heat.

Table S1. The pitch, bar width, hole size of Cu shadow mask with the mesh size of 200 – 2000.

Mesh size	Pitch (μm)	Bar width (μm)	Hole size (μm)
200	**125**	**30**	**70**
400	62	25	37
600	42	6	36
1000	25	6	19
1500	16.5	6	10.5
2000	12.5	6	6.5

The sensing materials, operation mode, operation temperature (*T*), power consumption (*P*), NO_2 concentration (*C*) and sensitivity (*S*) of chemiresistors operating at external heating mode (MEMS) and self-heating mode are listed in Table S2.

Table S2. Comparison of the characteristic parameters for chemiresistors operating at external heating mode (MEMS) and self-heating mode toward NO_2 from previous reports and the present work.

Materials	operation mode	*T* (°C)	*P*	*C* (ppm)	*S*	Ref.
a-Fe_2O_3/C mesoporous nanorods	MEMS	225	-	2.5	1.5	1
ZnO–CuO nanoflakes	MEMS	300	~120 mW	5	1.25	2
Au/SnO_2:NiO thin films	MEMS	500	-	5	185	3
WO_3	MEMS	300	65 mW (600 °C)	0.1	6.25	4
Au/Co_3O_4 nanoparticles	MEMS	136	11.2 mW	0.1	1.33	5
CuO-NWS	MEMS	119	-	0.2	1.4	6
WO_3 nanorods	MEMS	225	80 mW	10	2.02	7
CuO Nanosheets	MEMS	180	-	0.05	2	8
3D Ag-rGO	MEMS	133	52.8 mW	5	1.25	9
WO_3 nanoparticles	MEMS	205	23.4 mW	1	18.4	10
ZnO-NWs	MEMS	-	184 μW	1	7.05	11
ZnO nanorods	MEMS	-	22 mW	5	~77	12
SnO_2 nanoparticles and MWCNTs	MEMS	300	47.6 mW	3.6	4	13
carbon nanotube	Self-heating	-	2.9 μW	0.9	~1.9	14
SnO_2 NWs	Self-heating	175	25 mW	2.5	25.6	15
Au/ZnO NWs	Self-heating	-	0.37 mW	10	2.9	16
SnO_2 NWs	Self-heating	-	1 μW	0.1	1.1	17
nanocolumnar WO_3 film	Self-heating	~120	21.6 μW	1	~13	18
SnO_2 NW	Self-heating	-	35 μW	1	~3	19
Single SnO_2 NW	Self-heating	-	1.6 μW	0.1	3	20
$W_{18}O_{49}$ NWs	Self-heating	-	0.13 μW	5	24.6	This work

Table S3 showed that the sensing parameters of WO_x based chemiresistors on external heating mode such as sensing materials, operation temperature (*T*), NO_2 concentration (*C*), response/ recovery time (t_{res}/t_{rec}), sensitivity (*S*) and limit of detection (LoD).

Table S3. Comparison of the characteristic parameters for WO_x based chemiresistors toward NO_2 from previous reports and the present work.

Materials	*T* (ºC)	*C* (ppm)	t_{res}/t_{rec} (s)	*S*	LoD (ppm)	Ref.
WO_{3-x} NWs	100	10	-	57.9	-	21
WO_3 nanoplates	100	100	~50/-	131.8	1	22
WO_3 NWs	250	5	-	1.9	-	23
Pt/$W_{18}O_{49}$ NWs	94	100	-	4039.1	-	24
WO_3 nanoparticles	50	10	63/28	842.7	-	10
Pt/WO_3 thin films	300	4	-	25	0.5	25
Ag/WO_3	200	3		~12.2	0.1	26
C-WO_3	150	10	-	206	-	27
NiO/$NiWO_4$/WO_3 NWs	300	1	-	~25	-	28
Si/WO_3 NWs	200	10	~170/-	1.5	-	29
IrO_2-loaded WO_3 NWs	200	1	-	~275	<0.25	30
Sb/WO_3	70	5	70/50	1420	0.5	31
graphene/$W_{18}O_{49}$ nanowire aerogels	140	0.975	-	~1.3	0.2	32
WO_X nanosheet	200	0.5	-	~8	0.1	33
Sn-doped WO_3	100	0.1	249/519	~55	0.005	34
WO_3-$W_{18}O_{49}$	250	500	-	~12	-	35
Au-modified PS/WO_3	25	1	-	~5	-	36
Si nanowires/WO_3 NWs	25	2	-	~2.8	-	37
hexagonal WO_3	250	50	-	44	-	38
WO_3 lamellae	200	1	-	250	20	39
Bridged WO_3 NWs	200	5	-	1089.7	5 ppb	This work

References

1. L. Y. Zhu, K. Yuan, Z. C. Li, X. Y. Miao, J. C. Wang, S. Sun, A. Devi and H. L. Lu, *J. Colloid Interface Sci.*, 2022, **622**, 156-168.
2. B. Behera and S. Chandra, *Sens. Actuators, B*, 2016, **229**, 414-424.
3. Y. Wang, C. Liu, Z. Wang, Z. Song, X. Zhou, N. Han and Y. Chen, *Sens. Actuators, B*, 2019, **278**, 28-38.
4. B. Urasinska-Wojcik, T. A. Vincent, M. F. Chowdhury and J. W. Gardner, *Sens. Actuators, B*, 2017, **239**, 1051-1059.
5. T.-J. Hsueh and S.-S. Wu, *Sens. Actuators, B*, 2021, **329**, 129201.
6. T.-J. Hsueh, P.-S. Li, S.-Y. Fang and C.-L. Hsu, *Sens. Actuators, B*, 2022, **355**, 131260.
7. B. Behera and S. Chandra, *Mater. Sci. Semicond. Process.*, 2018, **86**, 79-84.
8. J.-L. Hou and T.-J. Hsueh, *ACS Appl. Electron. Mater.*, 2021, **3**, 4817-4823.
9. Q. Li, D. Chen, J. Miao, S. Lin, Z. Yu, Y. Han, Z. Yang, X. Zhi, D. Cui and Z. An, *ACS Appl. Mater. Interfaces*, 2020, **12**, 25243-25252.
10. T. Dai, G. Meng, Z. Deng, Y. Chen, H. Liu, L. Li, S. Wang, J. Chang, P. Xu, X. Li and X. Fang, *ACS Appl. Mater. Interfaces*, 2020, **12**, 37295-37304.
11. I. Cho, Y. C. Sim, M. Cho, Y. H. Cho and I. Park, *ACS Sens.*, 2020, **5**, 563-570.
12. S. J. Park, J. Park, H. Y. Lee, S. E. Moon, K. H. Park, J. Kim, S. Maeng, F. Udrea, W. I. Milne and G. T. Kim, *J. Nanosci. Nanotechnol.*, 2010, **10**, 3385-3388.
13. K.-Y. Choi, J.-S. Park, K.-B. Park, H. J. Kim, H.-D. Park and S.-D. Kim, *Sens. Actuators, B*, 2010, **150**, 65-72.
14. K. Chikkadi, M. Muoth, V. Maiwald, C. Roman and C. Hierold, *Appl. Phys. Lett.*, 2013, **103**, 223109.
15. H. M. Tan, C. Manh Hung, T. M. Ngoc, H. Nguyen, N. Duc Hoa, N. Van Duy and N. V. Hieu, *ACS Appl. Mater. Interfaces*, 2017, **9**, 6153-6162.
16. J. H. Kim, A. Mirzaei, H. W. Kim and S. S. Kim, *ACS Appl. Mater. Interfaces*, 2019, **11**, 24172-24183.
17. T. M. Ngoc, N. Van Duy, C. M. Hung, N. D. Hoa, N. N. Trung, H. Nguyen and N. Van Hieu, *RSC Adv.*, 2018, **8**, 36323-36330.

18. H. G. Moon, Y. S. Shim, D. H. Kim, H. Y. Jeong, M. Jeong, J. Y. Jung, S. M. Han, J. K. Kim, J. S. Kim, H. H. Park, J. H. Lee, H. L. Tuller, S. J. Yoon and H. W. Jang, *Sci. Rep.*, 2012, **2**, 588.
19. N. D. Chinh, N. Van Toan, V. Van Quang, N. Van Duy, N. D. Hoa and N. Van Hieu, *Sens. Actuators, B*, 2014, **201**, 7-12.
20. G. Meng, F. Zhuge, K. Nagashima, A. Nakao, M. Kanai, Y. He, M. Boudot, T. Takahashi, K. Uchida and T. Yanagida, *ACS Sens.*, 2016, **1**, 997-1002.
21. N. Lu, C. Yang, P. Liu and X. Su, *J. Colloid Interface Sci.*, 2019, **557**, 311-317.
22. S. S. Shendage, V. L. Patil, S. A. Vanalakar, S. P. Patil, N. S. Harale, J. L. Bhosale, J. H. Kim and P. S. Patil, *Sens. Actuators, B*, 2017, **240**, 426-433.
23. O. Chmela, J. Sadilek, G. Domenech-Gil, J. Sama, J. Somer, R. Mohan, A. Romano-Rodriguez, J. Hubalek and S. Vallejos, *Nanoscale*, 2018, **10**, 9087-9096.
24. T. Dai, Z. Deng, S. Wang, X. Fang and G. Meng, *Nanoscale*, 2022, **14**, 5002-5009.
25. Q. A. Drmosh, Y. A. A. Wajih, R. Al-Rammah, M. Qamar and Z. H. Yamani, *Appl. Surf. Sci.*, 2020, **517**, 146235.
26. C. Kamble, M. Panse and A. Nimbalkar, *Mater. Sci. Semicond. Process.*, 2019, **103**, 104613.
27. Y. Kang, D. Baek, S. Pyo and J. Kim, *IEEE Sens. J.*, 2020, **20**, 5705-5711.
28. N. Kaur, D. Zappa, V. A. Maraloiu and E. Comini, *Adv. Funct. Mater.*, 2021, **31**, 2104416.
29. K. Lee, D.-H. Baek, H. Na, J. Choi and J. Kim, *Sens. Actuators, B*, 2018, **265**, 522-528.
30. E. Navarrete, C. Bittencourt, P. Umek, D. Cossement, F. Güell and E. Llobet, *J. Alloys Compd.*, 2020, **812**, 152156.
31. J. Qi, K. Chen, Y. Xing, H. Fan, H. Zhao, J. Yang, L. Li, B. Yan, J. Zhou, L. Guo and S. Yang, *Nanoscale*, 2018, **10**, 7440-7450.
32. G. Shao, O. Ovsianytskyi, M. F. Bekheet and A. Gurlo, *Chem. Commun.*, 2020, **56**, 450-453.
33. D. T. Thu, D. V. Huong, P. Q. Ngan, G. H. Thai, D. T. A. Thu, N. N. Toan, H. T. Giang and N. T. Huy, *J. Nanosci. Nanotechnol.*, 2016, **16**, 7935-7941.
34. C. Wang, L. Guo, N. Xie, X. Kou, Y. Sun, X. Chuai, S. Zhang, H. Song, Y. Wang and G. Lu, *J. Colloid Interface Sci.*, 2018, **512**, 740-749.
35. Y. Xiong, Z. Zhu, T. Guo, H. Li and Q. Xue, *J. Hazard. Mater.*, 2018, **353**, 290-299.
36. L. Yuan, M. Hu, Y. Wei and W. Ma, *Appl. Surf. Sci.*, 2016, **389**, 824-834.

37. W. Zhang, M. Hu, X. Liu, Y. Wei, N. Li and Y. Qin, *J. Alloys Compd.*, 2016, **679**, 391-399.

38. Y. Zhang, W. Zeng and Y. Li, *Ceram. Int.*, 2019, **45**, 6043-6050.

39. T. Kida, A. Nishiyama, Z. Hua, K. Suematsu, M. Yuasa and K. Shimanoe, *Langmuir*, 2014, **30**, 2571-2579.